P- ISSN 1991-8941 E-ISSN 2706-6703
2025,(19), (01):174 – 190

Journal of University of Anbar for Pure Science (JUAPS) Open Access

Semi-automated analysis for nanoscale determination of chlorpheniramine maleate drug by using sodium nitroprusside by continuous flow feed via homemade NAG-SSP photometer

Nagham S. Turkey Al-Awadie , Asma A. Gayed Al-Ani *

Department of Chemistry, College of Science, University of Baghdad, Baghdad, Iraq;

ARTICLE INFO

Received: 13 / 05 /2024
Accepted: 05/ 09 /2024
Available online: 21/ 06 /2025

DOI: 10.37652/juaps.2024.149815.1259

Keywords:
CFIA, Turbidity, sodium nitroprusside, chlorpheniramine maleate, NAG-SSP-5S-1D Analyzer, Spectrophotometric method.

ABSTRACT

This study presents a rapid, sensitive, and straightforward approach to measure chlorpheniramine maleate (CPM) by using turbidity CFIA. The method involves CPM reacting with sodium nitroprusside (Nitropress) to produce a pale white precipitate. The NAG-SSP-5S-1D analyzer was used to measure turbidity at 0°–180° angle to detect the attenuation of incident light as a result of collision on the surfaces of the precipitate particles.

The linear range of CPM measurements was between 0.008 and 11 m.mol/L, with correlation coefficient of 0.9983 and R^2% = 99.65. The limit of detection was determined to be 0.0328 µg/sample from the lowest concentration in the calibration curve, and the repeatability of the method (RSD%) was less than 0.4% (n = 6) for the selected concentration (10–13 m.mol/L). The method was successfully applied for the determination of CPM in various drugs by using the standard addition method. The developed method and the classical method (UV spectrophotometry at λ_{max}= 265 nm and turbidity) were compared using t-test. No significant difference was observed among the three methods at 95% confidence level. Overall, the developed flow injection method offers simplicity, sensitivity, and reliable analytical performance for the determination of CPM. This method can be used as an alternative for the analysis of CPM in drugs compared with the reference method.

Introduction

Chlorpheniramine maleate (CPM, Fig. 1) has a formula of $C_{16}H_{19}ClN_2.C_4H_4O_4$, a molecular weight of 390.9, and an IUPAC name of (*Z*)-but-2-enedioic acid;3-(4-chlorophenyl)-*N*,*N*-dimethyl-3-pyridin-2-ylpropan-1-amine. It is white, odorless, and a crystalline powder, with pH ranging from 4 to 5.

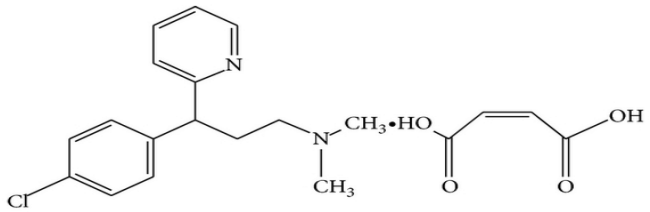

Fig. (1): Chlorpheniramine maleate structure.

CPM is an antihistamine medicine that relieves the symptoms of allergies. It is known as a drowsy (sedating) antihistamine, indicating that it is likely to make you feel sleepier than some other antihistamines[1].

*Corresponding author at : Department of Chemistry, College of Science, University of Baghdad, Baghdad, Iraq
ORCID: https://orcid.org/0009-0005-5916-2834 ,
Tel: +964 7819582931
Email: asma.alani.16@gmail.com

CPM relieves red, itchy, watery eyes; sneezing; itchy nose or throat; and runny nose caused by allergies, hay fever, and common colds. It is well absorbed after oral administration and has a serum half-life of approximately 20 h in adults. Food consumption slows the peak blood concentration of the drug but does not affect its absorption[2,3].

CPM belongs to first-generation antihistamines, and it is used to help alleviate symptoms of allergic reactions potentiated by histamine release. It is commonly used in small-animal veterinary medicine for its antihistaminic/antipruritic effects, especially for the treatment of pruritus in cats and occasionally as a mild sedative[4,5]. It enhances the efficacy of chloroquine in acute uncomplicated falciparum malaria. The adverse effects include drowsiness, dizziness, confusion, constipation, anxiety, nausea, blurred vision, restlessness, decreased coordination, dry mouth, shallow breathing, hallucinations, irritability, problems with memory or concentration, tinnitus, and trouble urinating[6,7].

One of the most practical and adaptable automated analysis methods is flow injection analysis

(FIA), which is extensively used for regular analyses across a range of industries[8]. It is used for chemical analysis. A sample plug is injected into a moving carrier stream to obtain the desired result. A sample is injected into a flowing carrier solution that mixes with reagents before reaching a detector in FIA[9,10]. It has several application in different media[11–16].

Several methods have been described for the simultaneous quantitative determination of CPM, including high-performance liquid chromatography (HPLC), carbon paste electrodes modified by nanoparticles[17,25], UV spectrophotometry[26,32], FIA[33], gas chromatography [34–38], and liquid chromatography[39–42].

This paper outlines a technique for detecting CPM in different drugs by using continuous FIA through turbidimetric measurements. Nitropress was used as a precipitating reagent in an aqueous medium. The precipitate was measured by the attenuation of incident light at 0°–180° angles by using the NAG-SSP-5S-1D analyzer[43], which is based on the flow cell receiving radiation from five irradiation sources. Each source irradiated a spot with a diameter of 5 mm, based on the 4 mm inner and 6 mm outer diameter of the flow tube. Therefore, 5 mm was taken as an irradiation spot to avoid loss and provide a widened scope for receiving the energy applied to the precipitate particles and expanding it to include attenuation measurement, deviation, and diffraction of incident light. This characteristic is available in the NAG-SSP-5S-1D analyzer.

The analytical response for each concentration was recorded over time. The results were compared with the reference UV–Vis spectrophotometric and turbidity methods.

Materials and Methods

CPM and the precipitating agent Nitropress were prepared. Distilled water was chosen to prepare 0.25 M acids (HCL, HNO_3, H_2SO_4, CH_3COOH, H_3PO_4) and salts (NaCl, KCl, CH_3COONH_4, and NH_4Cl) in a 250 ml volumetric flask. The acids were calibrated using a standard solution of sodium carbonate and used in the experiment to determine the optimal chemical conditions.

Methodology

NAG-SSP-5S-1D is a unique instrument made at home. It represents a flow cell, which is composed of two parts: middle region with a 55 mm length of exposure to irradiation and detection with 25 mm sides from each side, which represents a path length of 4 mm. SSP represents the simplest, sensitive, and portable instrument to measure the attenuation 0 photon light. The sources are a five white snow light emitting diode (WSLED), symbolized by 5WSLED or 5S, and one detector of solar cell, symbolized by1D. A selector control knob of variable light intensity can be applied as a request in accordance with the variable optimization of reaction parameters for any specific reaction. Colloidal and crystalline precipitated particulates can be handled. The reaction of CPM with Nitropress gives a pale yellow precipitate [44], as shown in Scheme 1, to asses CPM in drugs. Fig. 1 shows a flow diagram of the manifold used for this determination of CPM. A two-line system was used (Fig. 2) with the NAG-SSP-5S-1D analyzer[43] using the optimal parameters of the CPM-Nitropress (2 m.mol/L) system. A sample volume of 120 µL was injected on a carrier stream line (distilled water) at 1.7 $ml.min^{-1}$ and 3.0 VDC. The precipitate was expected to be probably pale white, as shown in the suggested reaction in Scheme 1[44].

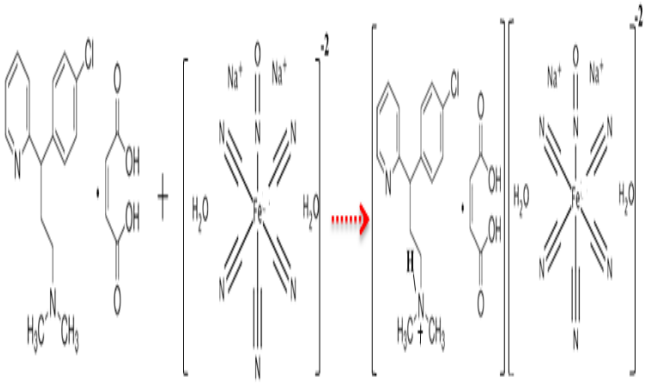

Chlorpheniramine maleate **$Na_2Fe(CN)_5NO.2H_2O$ pale white precipitate**

Scheme 1: Reaction between CPM with Nitropress and pale white precipitate.

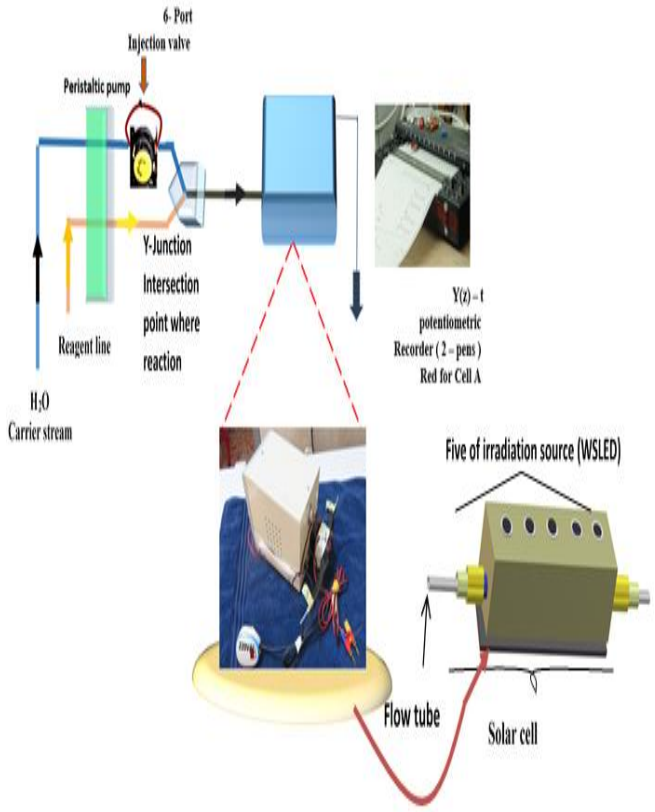

Fig. 2: Diagram of the manifold for assessment of NAG-SSP-5S-1D analyzer via reaction of CPM (10 m.mol/L)with Nitropress (2 m.mol/L).

Results and discussion

Optimization of chemical and physical parameters

The optimal conditions for choosing the best (S/N) profile measured at 0°–180° were investigated. A series of physical and chemical parameters was optimized inside the manifold system.

Chemical parameters

The chemical parameters included the precipitate agent and the medium of reaction (acids and salts).

Effect of variable concentration of sodium nitroprusside

At the range of 0.5–6 m.mol/L and 1.6 ml/min, the impact of changing the concentration of Nitropress as a precipitate reagent was investigated. The sample volume was 85 µL, open valve, without coil, 3.1 VDC, and a CPM concentration of 10 m.mol/L was employed.

Fig. 3.A shows that the responses showed an increase in light attenuation and in the concentration of the precipitating agent, which, in turn, may lead to an increase in the density and growth of the crystals and their compactness with another, while providing some interstitial spaces to allow the remaining light to penetrate towards the detector, reaching 2 m.mol/L. An increase in concentration, (i.e., larger than 2 m.mol/L, Fig. 3.B) led to responses at low height, which is likely due to the agglomeration of particles, large size, and their deposition or retention of impurities or water particles, resulting in a decrease in light attenuation. On this basis, 2 m.mol/L was the optimal concentration, matching the chosen segment of the slope-intercept method. S_2 is the ideal segment within which the concentration is 2 m.mol/L. This finding indicated that any concentration can be used within this segment, resulting in approximately the same sensitivity. The results are summarized in Tables 1A and B and Fig. 2.B. The ideal concentration for use in future work is 2 m.mol/L of Nitropress.

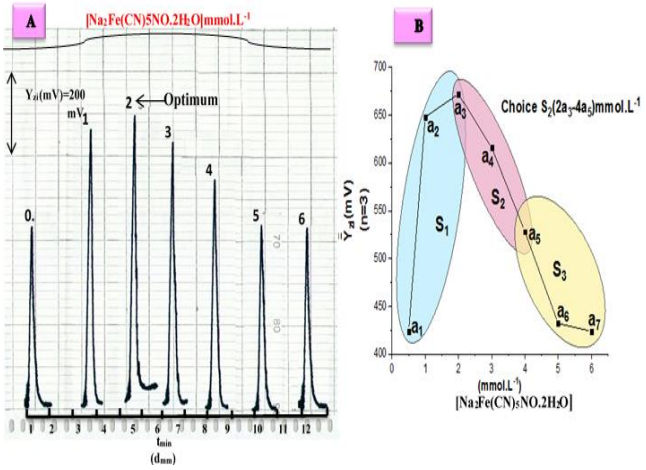

$\bar{Y}_{Zi}$(mV) Average output response of NAG-SSP-5S-1D analyzer

Fig. 3.A: Response profile of Nitropress concentration effect.
B: $\bar{Y}_{Zi}$(mV) Average output response of NAG-SSP-5S-1D analyzer and three data points as one segment with optimal choice.

Table 1. A: Effect of Nitropress
B: Mode of segmentation

A	
Type of system	
CPM (10mmol.L^{-1})-Nitropress system, 3.1 VDC, 85 µL, 1.6 ml.min^{-1}	
Type of precipitating agent	Reliability at 95% confidence level (RSD%)$\bar{Y}_{zi}$ (mV)(n = 3) $\pm t_{0.05/2,2} \frac{\sigma n-1}{\sqrt{n}}$
$Na_2Fe(CN)_5NO.2H_2O$]mmol.L^{-1}	
0.5	2.782 (0.264) 424±
1	3.056 (0.189) 648±
2	2.981 (0.179) 672±
3	2.683 (0.175) 616±

4				2.509	(0.191) 528±
5				2.758	(0.257) 432±
6				3.528	(0.335) 424±
B					
Segment	Range of [PHMA]mmol.L^{-1}	Intercept(a) mV	Slope(b) mV/mmol.L^{-1}	Correlation Coefficient (r)	(Ø)
S_1	0.5-2	412	145.143	0.810	89.6
S_2	2-4	821.3	-72	0.992	-89.2
S_3	4-6	721.3	-52	0.899	-88.9

$\bar{Y}_{zi}$(mV): Average output response of NAG-SSP-5S-1D analyzer, 95% confidence level, $t_{0.025,2}$ = 4.303.

Effect of media (acids and salts)

This study was conducted on the basis that the crystal structure of a mobile system in the manifold of continuous flow injection techniques is of different shapes, thus obtaining crystal growth of particles of small sizes and scattered non-compact ones (nuclei formation) and unable to attenuate incident light. Any change in the deposition medium may lead to improving crystal growth, overcoming charge repulsion, and encouraging the condensation of nuclei by adding some salts or acids to rebuild the crystal structure in a purer form. So, the CPM (10 m.mol/L) with Nitropress (2 m.mol/L) was studied at various salts and acids at a concentration of 10 m.mol/L, with a sample volume of 85 µL, without coil, open valve, and a flow rate of 1.6 ml.min^{-1} for both lines. Fig. 4.A. displays the obtained profile. Table 2 provides a summary of the data, showing the transducer energy response varied with different mediums and was expressed as an average peak heights (n = 3) in mV. Every acid resulted in a drop in the responses. This finding could be related to the precipitate's formation during the peptization process or to the solid particulate's dissolution, which lowers the precipitate's dense mass. So, compared with acids and salts, distilled water is preferable as a carrier stream because it may have contributed to the formation of compact crystals that act as reflective surfaces, scattering of light or attenuation of incident light by reducing the gaps between the deposited particles and causing agglomeration, leading to an increase in large particles and thus achieving the granulation stage. On this basis, distilled water as a carrier stream is most suitable for obtaining responses of maximum attenuation of incident light (Fig. 4.B).

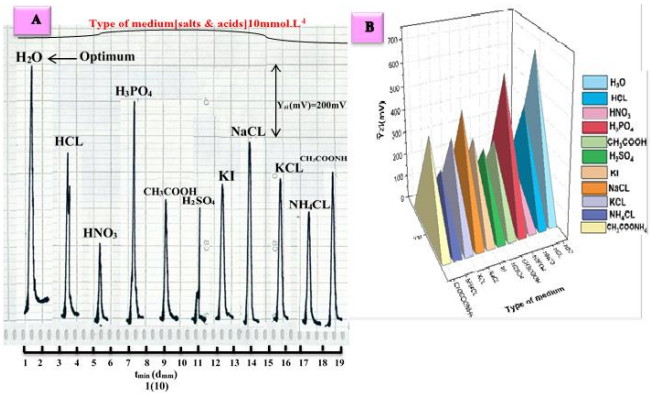

Y_{zi}(mV): Output profile of NAG-SSP-5S-1D analyzer, $\bar{Y}_{zi}$(mV): Average output response of NAG-SSP-5S-1D analyzer.

Fig. 4: Effect of salts and acids on (A) response profile.
B: Mode of segmentation

Table 2: Effect of different media on the precipitation of CPM (10 m.mol/L) with Nitropress (2 m.mol/L)

Type of system		
CPM (10 mmol.L^{-1})-Nitropress (2 mmol.L^{-1}) system, 3.1 VDC, 85 µL, 1.6 ml.min^{-1}		
Type of medium	Reliability at 95% confidence level (RSD%) $\bar{Y}_{zi}$(mV, n = 3) ± $t_{0.05/2,2}$ $\frac{\sigma n-1}{\sqrt{n}}$	
Salt or H_3O^+ 10 mmol.L^{-1}		
H_2O	3.279	(0.196) 672±
HCL	3.677	(0.330) 448±
HNO_3	3.627	(0.702) 208±
H_3PO_4	3.453	(0.232)600±
CH_3COOH	4.273	(0.524) 328±
H_2SO_4	4.049	(0.536) 304±
KI	3.776	(0.422)360±
NaCL	± 3.304	(0.273) 488
KCL	± 3.528	(0.369) 384
NH_4CL	3.751	(0.572)264±
CH_3COONH_4	3.031	(0.293)416±

$\bar{Y}_{Zi}$(mV): Average output response of NAG-SSP-5S-1D analyzer, $t_{0.05/2,n-1}$ = 4.303, 95% confidence level.

Physical parameters

Intensity irradiation source

Under the experimental conditions of CPM (10 m.mol/L) with Nitropress (2 m.mol/L) with 85 µl of sample volume, without coil, open valve, and 1.6 ml.min^{-1} of flow rate, the variable intensity of irradiation source was applied. Fig. 2 shows the front panel of the sophisticated digital DC power, which includes the ON-OFF operation switches, in addition to

the voltage changing switches for the 0–15 VDC supply, which were used to change the light intensity of the light emitting diodes. The profile and results are shown in Fig. 5.A and Table 3.A. An increase in the height of the response was observed with increasing voltages supplied to the irradiation sources to match the density and quantity of the precipitate particles transverse in front of the detector, up to 3.0 VDC. Above 3.0 VDC, a decrease in the height of the response was observed.

This finding is likely due to the high light intensity causing an increase in the number of photons due to the reflection of optical fibers, which causes transparency in the particles present, and the surfaces of the particles are not able to attenuate the incident light, leading to a decrease in the height of responses. This phenomenon is very important in the case of the filtration process and purifying signals from noise. The best voltage to obtain high sensitivity and maintain the life of the irradiation source was 3.0 VDC, and these results corresponded with the slope-intercept method. S_4 (i.e.; 3.0-3.2 VDC) is segment show. Table 3.B. shows that choice $S_4(3.0a_6- 3.2a_8)$VDC with confident. So, the optimal irradiation source intensity was 3.0 VDC.

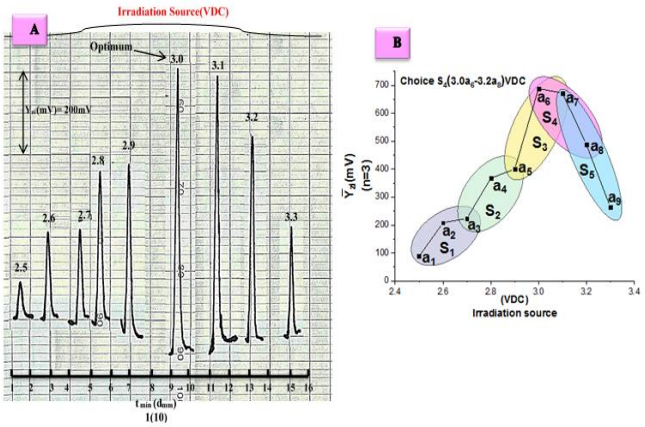

Y_{zi}(mV): Output profile of NAG-SSP-5S-1D Analyzer,
$\bar{Y}_{zi}$(mV):Average output response of NAG-SSP-5S-1D Analyzer.

Fig. 5: Effect of intensity of irradiation source on :A: peak height of response- time.
B: Mode of segmentation

Table 3. A.: Effect of intensity
B: Mode of segmentation

A	
Type of system	
CPM (10 mmol.L^{-1})-Nitropress (2mmol.L^{-1}) system, 85 µL, 1.6 ml.min^{-1}	
Intensity VDC	Reliability at 95% confident level (RSD%) $\bar{Y}_{zi}$(mV)(n=3)±$t_{0.05/2,2}\frac{\sigma n-1}{\sqrt{n}}$
2.5	2.832 (1.295)± 88
2.6	3.056 (0.591)208±
2.7	2.758 (0.496) 224±
2.8	3.553 (0.389)368±
2.9	2.708 (0.273) 400±
3.0	2.832 (0.166)688±
3.1	3.776 (0.226)672±
3.2	488 ± 3.031 (0.250)
3.3	264 ± 3.056 (0.466)

B

Segment	Intensity of irradiation source VDC	Intercept(a) mV	Slope(b) mV/mmol.L^{-1}	Correlation coefficient (r)	Angle Ø)(
S_1	2.5-2.7	-1594.67	680	0.915	89.9
S_2	2.7-2.9	-2133.3	880	0.939	89.9
S_3	2.9-3.1	-3493.3	1360	0.840	89.9
S_4	3.0-3.2	3716	-1000	0.899	-89.94
S_5	3.1-3.3	7002.67	-2040	0.998	-89.97

$\bar{Y}_{Zi}$(mV): Average output response of NAG-SSP-5S-1D analyzer, $t_{0.05/2,n-1}$ = 4.303, 95% confidence level.

Effect of flow rate

CPM (10 m.mol/L) with Nitropress (2 m.mol/L) was employed, and the flow rate was varied, ranging from 0.5 ml.min^{-1} to 2.5 ml.min^{-1}, for the reagent and carrier stream, respectively. The sample segment was , 85 µL, open valve, without coil, and 3.0 VDC intensity of light. The response profile shown in Fig. 6.A is distorted, especially at low flow rate, giving enough time for growth causing an increase in peak height. When the speed increased, regular responses were obtained, sharp and not broad at the base. On this basis, the 1.7 ml.min^{-1} flow rate for both lines was chosen for the subsequent experiments. The obtained confidence corresponded with the slope-intercept method for the choice of optimal parameters (Tables 4.A and B). Sector S_4 (i.e., 1.7–2.3 ml.min^{-1}, Fig. 6.B) was the chosen section due to the increase in intercept (a) value, and 1.7 ml.min^{-1} was the optimal, falling within S_4.

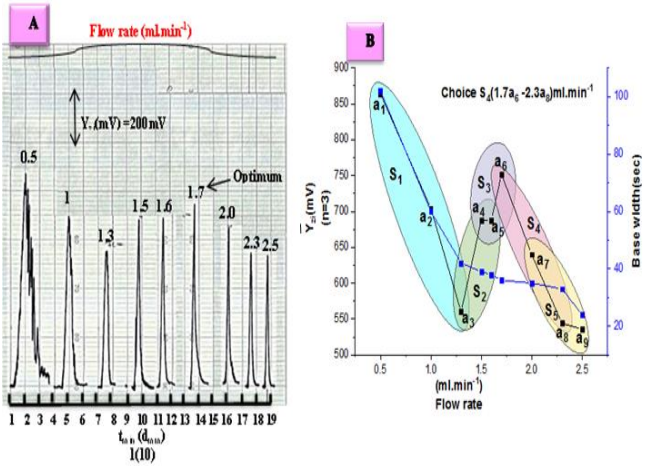

Y_{zi}(mV): Output profile of NAG-SSP-5S-1D analyzer ,$\bar{Y}_{zi}$(mV): Average output response of NAG-SSP-5S-1D analyzer.

Fig. 6.A: Effect of flow rate on the response profile.

B: Mode of segmentation.

Table 4.A: Flow rate effect.

B: Mode of segmentation

A				
Type of system				
CPM (10mmol.L^{-1})-Nitropress (2 mmol.L^{-1}) system, 3 VDC, 85 µL				
(pump speed)role/min Flow rate for each line ml.min^{-1}	Reliability at 95% confident level (RSD%) $\bar{Y}_{zi}$(mV)(n=3)±$t_{0.052,2}\frac{\sigma n-1}{\sqrt{n}}$		$\Delta t_{B(sec)}$ / V_{ml}	$C_{mmol.L^{-1}}$ / D_F
(5) 0.5	2.708	(0.126)864±	102 / 1.785	0.476 / 21.008
(10) 1	3.553	(0.203)704±	60 / 2.085	0.408 / 24.509
(15) 1.3	3.801	(0.273)560±	42 / 1.905	0.446 / 22.422
(20) 1.5	2.932	(0.172)688±	39 / 2.035	0.418 / 23.923
(25) 1.6	3.553	(0.208)688±	38 / 2.11	0.403 / 24.814
(27) 1.7	3.105	(0.166)752±	36 / 2.125	0.400 / 25.000
(30) 2.0	3.776	(0.238)640±	35 / 2.418	0.352 / 28.409
(35) 2.3	544± 3.677	(0.272)	33 / 2.615	0.325 / 30.769
(40) 2.5	536± 4.248	(0.319)	24 / 2.085	0.408 / 24.509

B					
Segment	Flow rate ml.min^{-1}	Intercept mV	Slope mV/ mmol.L^{-1}	correlation coefficient (r)	Angle tangent of slope
S_1	0.5-1.3	1058.286	-373.878	0.994	-89.8
S_2	1.3-1.6	-25.143	457.143	0.945	89.9
S_3	1.5-1.7	197.3	320	0.866	89.8
S_4	1.7-2.3	1338.67	-346.67	0.999	-89.8
S_5	2.0-2.5	1064.8	-216.842	0.943	-89.7

$\bar{Y}_{Zi}$(mV): Average response of NAG-SSP-5S-1D analyzer

Δt_B(sec): Base width of peak (sec), C: concentration at flow cell, D_f: dilution factor at flow cell, 95% confidence level.

Sample volume

Under 1.7 ml/min for both lines, CPM at 10 m.mol/L and Nitropress at 2 m.mol/L were used to study the variable length of Teflon tube (IØ = 1 mm) ranging from 3.2 to 25 cm, which is equivalent to 25–196 µL as a sample volume. The responses obtained (Fig. 7.A) included the relationship between Y_{zi}(mV) and time [$t_{min}(d_{mm})$], and the data are summed up in Table 5.A. The highest responses were obtained at 120 µL. A larger volume (> 120 µL) caused a decrease in the height of responses and an increase of Δt_B. This finding is mainly a dual effect: filtering on the output of responses and reducing the effect of attenuation of incident light. On this basis and the economy of sample segment, 120 µL was the best (Fig. 7.B), which falls within S_3 (a_5-a_7) with slope-intercept method (Table 5.B). It was selected because it gives the highest sensitivity due to the high value of intercept (a).

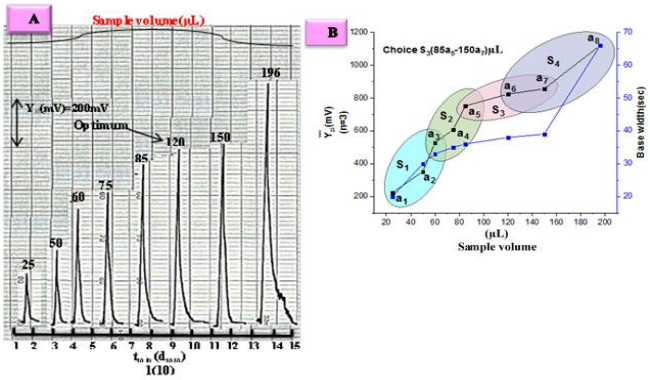

Y_{zi}(mV): Output profile of NAG-SSP-5S-1D analyzer. $\bar{Y}_{zi}$(mV): Average output response of NAG-SSP-5S-1D analyzer.

Fig. 7.A: Effect of sample volume on response profile.
B: Mode of segmentation

Table 5.A.: Effect of sample volume (SV)
B: Mode of segmentation

A				
Type of system				
CPM (10 mmol.L^{-1})-Nitropress (2 mmol.L^{-1}) system, 3 VDC, 1.7 ml.min^{-1}				
(Sample length-Cm) IØ=1mm Sample volume (µL)	Reliability at 95% confident level (RSD%) $\bar{Y}_{zi}$(mV)(n=3)±$t_{0.05,2,2}\frac{\sigma n-1}{\sqrt{n}}$		$\Delta t_{B(sec)}$ / V_{ml}	$C_{mmol.L^{-1}}$ / D_F
(3.2) 25	3.279	(0.589)224±	20 / 1.158	0.216 / 46.296
(6.4) 50	3.304	(0.378)352±	30 / 1.75	0.286 / 34.965
(7.7) 60	2.708	(0.206)528±	33 / 1.93	0.311 / 32.154
(9.6) 75	3.180	(0.211)608±	35 / 2.058	0.364 / 27.473
(10.8) 85	3.503	(0.188)752±	36 / 2.125	0.400 / 25.000
(15.3) 120	3.105	(0.152)824±	38 / 2.273	0.528 / 18.939
(19.1) 150	3.950	(0.186)856±	39 / 2.36	0.636 / 15.723
(25) 196	1120± 4.521	(0.163)	66 / 3.936	0.498 / 20.080

B					
Segment	Sample volume µL	Intercept mV	Slope(b) mV/mmol.L-1	correlation coefficient (r)	Angle tangent of slope (Ø)
S1	25-60	8	8	0.945	82.87
S2	60-85	-6.737	8.674	0.961	83.4
S3	85-150	619.843	1.613	0.985	58
S4	120-196	304.368	4.049	0.954	76

$\bar{Y}_{Zi}$ (mV): (S/N) energy transducer response in mV, Δt_B (sec) : base width of peak (sec), C*: concentration at flow cell of NAG-SSP-5S-1D analyzer, Df: dilution factor at flow cell, V*: volume at flow cell of NAG-SSP-5S-1D analyzer, 95% confidence level.

Effect of delay reaction coil

A flow rate of 1.7 ml.min^{-1} for both lines was used in a system of Nitropress (2 m.mol/L) and CPM (10 m.mol/L) with different coil volumes. Figs. 8.A and B show that an increase of coil volume led to a decrease in peak height, obtaining distorted responses as the signal descends to the baseline. In addition to the width of the base, which is most probably due to agglomeration and condensation of their masses and its difficulty in being moving with the carrier stream flow. The reaction between CPM and Nitropress was complete, with mixing coil of 314 µL in length, as shown in Fig. 8.A. All the data results are tabulated in Table 6.A. The enhanced sensitivity and the obtained data measurements showed that 314 µL had good excellent output. On this basis and supported by the slope-intercept method (Fig. 8.B and Table 6.B), segment number 2 was the best selected segment, falling the point (a_2) where the reaction coil is 314 µL, and it was used for further experiments.

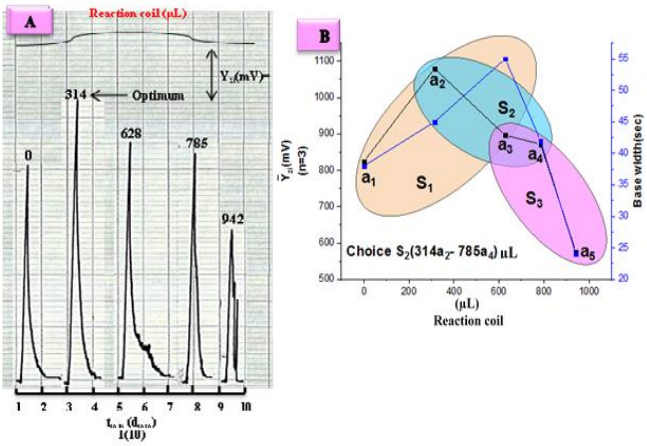

Y_{zi}(mV): Output profile of NAG-SSP-5S-1D analyzer, $\bar{Y}_{zi}$(mV): Average output response of NAG-SSP-5S-1D analyzer.

Fig. 8.A: Reaction coil effect on response profile
B: Mode of segmentation

Table 6.A: Effect of reaction coil.
B: Mode of segmentation

A				
Type of system				
CPM (10 mmol.L^{-1})-Nitropress (2 mmol.L^{-1}) system, 3 VDC, 120 µL, 1.7 ml.min^{-1}				
Reaction coil IØ=2mm (Cm) µL	Reliability at 95% confident level (RSD%) $\bar{Y}_{zi}$(mV)(n=3)±$t_{0.05,2,2}\frac{\sigma n-1}{\sqrt{n}}$		$\Delta t_{B(sec)}$ / V_{ml}	$C_{mmol.L^{-1}}$ / D_F
W.C	3.279	(0.160)824±	38 / 2.27	0.529 / 18.904

(10) 314	4.546	(0.169)1080±	45	0.449
			2.67	22.272
(20) 628	3.627	(0.163)896±	55	0.370
			3.24	27.027
(25) 785	3.478	(0.161)872±	42	0.48
			2.50	20.833
(30) 942	3.776	(0.264)576±	24	0.811
			1.48	12.330

B

Segment	Coil volume µL	Intercept mV	Slope mV/mmol.L^{-1}	correlation coefficient (r)	Angle tangent of slope Ø
S_1	0-628	897.3	0.1146	0.273	6.5
S_2	314-785	1215.429	-0.462	0.974	-24.8
S_3	628-942	1581.3	-1.0191	0.898	-45.5

W.C.: without coil, R.C.: Reaction coil, $\bar{Y}_{Zi}$(mV):(S/N) energy transducer response in mV, Δt_B (sec) :Base width of peak (sec), D.f : Dilution factor at flow cell, $V_{f.c.}$, $C_{f.c.}$: Volume of flow cell, concentration of flow cell respectively, 95% as a confidence level.

Variation of chlorpheniramine maleate concentration with (S/N) obtained profile at (0-180°) leads to the linear dynamic range:

Using a steps included in conc. (studied at t_{min} (d_{mm}))as the x-axis opposite y_{zi}.(mV) (represent dependent variable) with optimum of chemicals (i.e., CPM with Nitropress (2m.mol/L)) and physical parameters; a series of CPM solutions ranging 0.008-20 were prepared to study a relationship between x-represented the independent variable versus y here represent dependent variable which mean a real measured responses will be leading to the Fig. 9.A, in which the profile of responses obtained is observed and Scatter plot as explained in Fig. 9.B. which gave a coefficient of determination 0.9262 and chosen linear dynamic range (Table 7, 0.008-11) at R^2% percentage capital R-squared = 99.65% (Fig. 9.B); in which, the height of response increased when the analyte of concentration is increased due to increase the density of the small precipitate particulates up to 11m.mol/L will cause to deviation of linearity of the calibration graph which is likely due to agglomeration of the precipitate particulates and compactness together within the flow cell forming particles of large size that act as a reflective mirror, increasing the number of photons due to the phenomenon of reflection and scattering from the surface of the particles, or internal refractions within these agglomerated particles, in addition to the phenomenon of optical fibers, which occurs in the presence of three media of different densities and refractive factors. Therefore, this effect will cause some sections or particulate of the reaction product to become transparent and reduce its effect on the attenuation of incident light. The results obtained tabulated in table 7.

The assessment evaluation of new methodology (NAG-5S x 1(WSLED)-1D solar cell Analyzer for determination of CPM using CPM with Nitropress(2m.mol/L) was compared with the available literature method[45,46], namely UV-Spectrophotometric method which was based on measurements of absorbance at λ_{max}= 265nm (Fig. 10.A) for the concentration between 0.005 and 2.5 m.mol/L (Fig. 10.B).

The scatter plot in Fig. 9.B shows the linear range of 0.005–1.4 m.mol/L, the correlation coefficient of 0.9954, and R^2% = 99.07% (n = 19).

Another classical method is turbidity, which compares the new method with scatter plot ranging from 0.007 m.mol/L to 4 m.mol/L (Fig. 10.C) and correlation coefficient of 0.9359 and R^2% = 87.61% (n = 16).

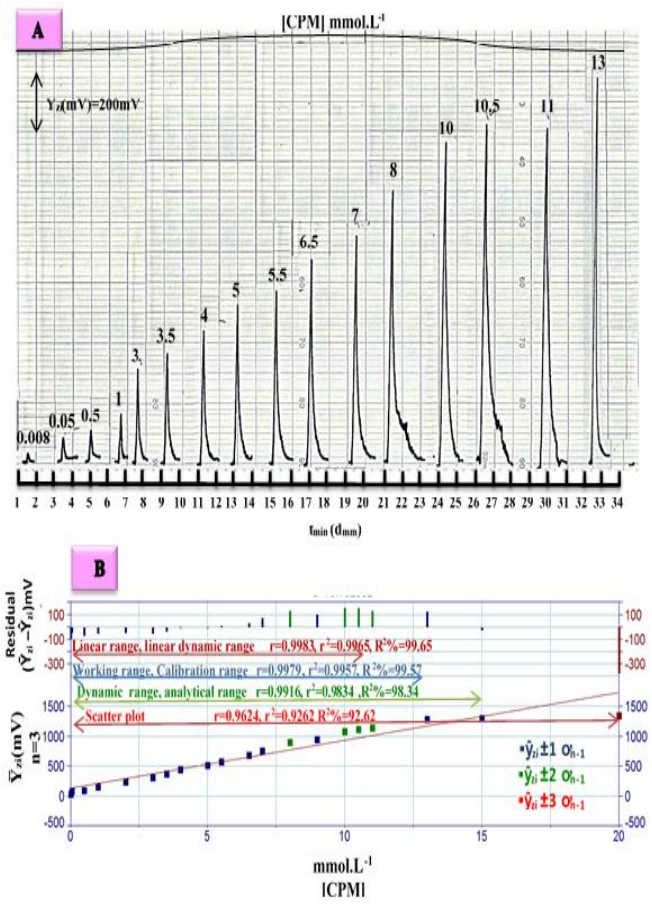

Y_{zi}(mV): Output profile of NAG-SSP-5S-1D Analyzer.
$\bar{Y}_{zi}$(mV):Average output response of NAG-SSP-5S-1D Analyzer.

Fig 9.A:Some of response profiles versus time. B:Variable range for the effect of CPM concentration on attenuation of incident light using NAG-SSP-5S-1D analyzer for linear range (0.008–11 m.mol/L), working range (0.008–13 m.mol/L), dynamic range (0.008–15 m.mol/L), and scatter plot (0.008–20 m.mol/L), using CPM with Nitropress (2 m.mol/L).

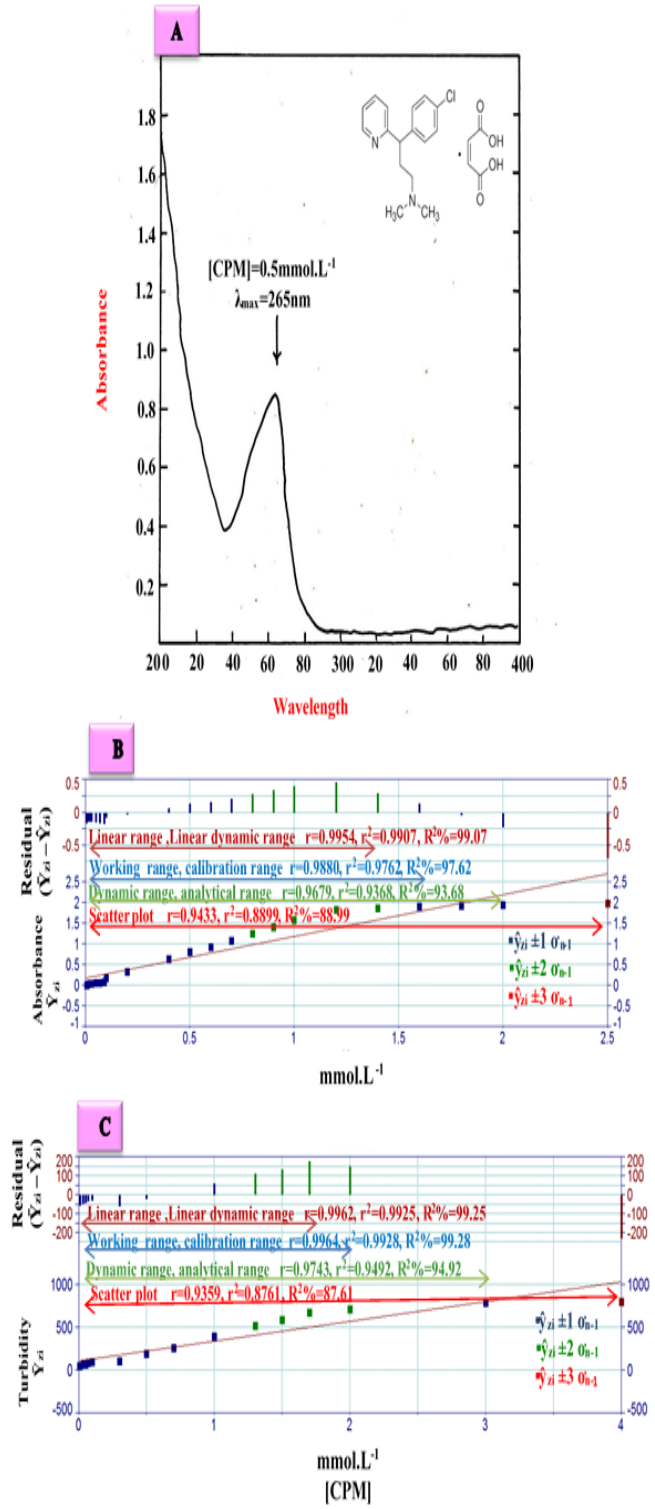

Fig. 10.A: UV–Vis absorbance spectra of CPM versus deionized water at λ_{max} = 265 nm. B: Linear range from 0.005 m.mol/L to 1.4 m.mol /L for n = 19 for CPM, in addition to working or calibration range from 0.005 m.mol/L to 1.6 m.mol/L for n = 20, dynamic range from 0.005 m.mol/L to 2 m.mol/L for n = 22, and scatter plots from 0.005 m.mol/L to 2.5 m.mol/L. Residual =($\bar{Y}_{zi}$ –$\hat{Y}_{zi}$) without unit on spectrophotometric method ,$\bar{Y}_{zi}$ = practical value without unit on spectrophotometric .

C: Turbidity method

Table 7: Summary of the findings for UV spectrometry and first-degree equation of the form Ŷ=a + b x at optimal co ndition linear regression for the fluctuation of (S/N) energy transducer response with CPM concentratio n.

Type of mode	Range of [CPM] mmol.L^{-1}(n)	$\hat{Y}_{zi}$=a± S_at+ b(Δy /ΔX mmol.L^{-1})± S_bt [CPM]mmol.L^{-1} _ 95% confidence level for n-2	r, r^2, R^2%	t_{tab}	Calculate d t-value t_{cal}=r/√n-2/ √1-r^2
CPM-Sodium nitroprusside (2 mmol.L^{-1}) system, 3 VDC, 1.7 ml.min^{-1}, 120 µL					
UV-spectrophotometer at λ_{max} = 265 nm.					
Turbidity method					
Linear range or linear dynamic range	0.008-11(17)	35.981±20.689+101.969±3.307[CPM]mmol.L^{-1}	0.9983, 0.9965,99.65	2.131<<65.701	
	0.005-1.4(19)	0.0183±0.044+1.484±0.074[CPM]mmol.L^{-1}	0.9954,0.9907 ,99.07	2.110 << 42.652	
	0.007-1.7(13)	45.037±16.989+360.192±20.793[CPM]mmol.L^{-1}	0.9962, 0.9925, 99.25	2.201<<38.128	
Working range or calibration range	0.008-13(18)	42.613±23.629+100.032±3.470[CPM]mmol.L^{-1}	0.9979, 0.9957, 99.57	2.120<<61.100	
	0.005-1.6(20)	0.045±0.074+1.379±0.107[CPM]mmol.L^{-1}	0.9880,0.9762 ,97.62	2.101 <<27.192	
	0.007-2(14)	47.940±17.948+350.905±18.859[CPM]mmol.L^{-1}	0.9964, 0.9928, 99.28	2.179<<40.543	
Dynamic range or analytical range	0.008-15(19)	65.495±46.781+94.115±6.265[CPM]mmol.L^{-1}	0.9916, 0.9834, 98.34	2.110<<31.695	
	0.005-2(22)	0.112±0.123+1.164±0.142[CPM]mmol.L^{-1}	0.9679,0.9368 ,93.68	2.086 << 17.214	
	0.007-3(15)	74.139±49.006+294.197±40.764[CPM]mmol.L^{-1}	0.9743, 0.9492, 94.92	2.160<<15.589	
Scatter plot	0.008-20(20)	131.964±95.287+79.793±11.154[CPM]mmol.L^{-1}	0.9624, 0.9262, 92.62	2.101<<15.029	
	0.005-2.5(23)	0.174±0.162+1.011±0.162[CPM]mmol.L^{-1}	0.9433,0.8899 ,88.99	2.080 << 13.026	
	0.007-4(16)	110.654±76.280+230.561±49.708[CPM]mmol.L^{-1}	0.9359, 0.8761, 87.61	2.145<<9.949	

$\hat{Y}_{zi}$=Estimated value, r: Correlation coefficient, r^2: Coefficient of determination, R^2% (percentage capital R-squared): Explained variation as a percentage /total variation, S_a: Standard deviation of intercept, S_b: Standard deviation of slope, t_{tab}= $t_{0.05/2,n-2}$.

Repeatability

The efficiency of the homemade NAG-5S X 1(WSLED)-1D solar cell analyzer was studied at a constant concentration of CPM (mainly two concentrations were mainly used) by using the optimal parameters [i.e., CPM (10 and 13 m.mol)–Nitropress (2 m.mol/L) system, 120 µL, 1.7 ml.min^{-1} flow rate, and 3.0 VDC as an intensity of irradiation source]. Six successive injections were measured (Fig. 11), and the results are tabulated in Table 8. The value of the percentage relative standard deviation was less than 0.4%, indicating that reliable measurements can be achieved using this method.

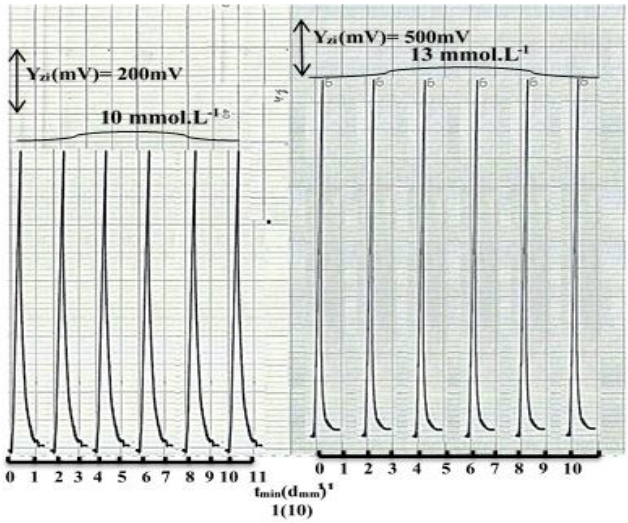

Y_{zi}(mV): Output profile of NAG-SSP-5S-1D analyzer.

Fig. 11: Y_{zi}(mV) – t_{min} (d_{mm}) background of six value for (10=13) m.mol/L concentration of CPM by Nitropress (2 m.mol/L), using 120 µL as injection of sample loop and 1.7 ml.min^{-1} flow rate for each line. High measurement repeatability at high sensitivity of using 200–500 mV.

Table 8: Repeatability of CPM.

[CPM] mmol.L^{-1}	Output response of NAG-SSP-5S-1D $\bar{Y}_{Zi}$.(mV) (n=6)	RSD %	Reliability (2- tail_ 95%) $\bar{Y}_{Zi}$.(mV)± $t_{0.05/2,n-1}$ $\frac{\sigma n-1}{\sqrt{n}}$
10	1080	0.23	1080 ± 2.607
13	1288	0.309	1288 ± 4.179

$\bar{Y}_{zi}$(mV):Average output response of NAG-SSP-5S-1D Analyzer, $t_{0.05/2,5}$=2.571 ,n=injection number.

Limit of detection (LOD)

The LOD of analyte in general may be described as the concentration that gives a signal y_{zi}(mV) significantly different from the blank signal. The LOD of CPM was determined via successive gradual dilution of the minimum concentration in the linear range of 0.008 m.mol/L. The LOD was 0.0328 µg/sample (0.0007 m.mol/L) of 120 µL as a sample volume. The LOD for CPM was calculated using three methods, as tabulated in Table 9.

Table 9:Detection limit of CPM

Practically based on the gradual dilution for the minimum concentration in scatter plot	Classical method	Classical meth

CPM-Nitro press System 0.0007 mmol.L^{-1}					
Newly developed method	Theoretical based on the value of slope $X=3S_b/slope$	Theoretical based on the linear equation $\hat{Y}=Y_b+3S_b$	Limit of quantitative L.O.Q $\hat{Y}=Y_b+10S_b$		
0.0328µg/sample	1.457 µg/sample	32.095 µg/sample	106.983 µg/sample	6.2544 µg/sample	20.718 µg/sample

$\hat{Y}$: Estimated response (mV), X: value of LOD based on the slope (depending on linear dynamic range), S_b: standard deviation of blank (n=16) equal to Sy/x (residual), (LOD depending on linear equation of linear range due to low Sy/x), Y_b: average response for blank = intercept (a).

Assessment of CPM in variable drugs by using NAG-5SX1(WSLED)-1D solar cell analyzer

The methodology and the instrument were evaluated on samples delivered from a local market and from different companies with the same amount of the active material (i.e. histadine, chlorohistol, and chlomal) by preparing a series of solutions extending from 0 to 8 m.mol/L from the standard drug of CPM (10 m.mol/L) in volumetric flask (10 ml) with the addition of constant volume of 2.5ml from each sample (three samples) for three methods i.e., the developed method of the NAG-SSP-5S-1D analyzer, the classical spectrophotometry at 265 nm using standard addition method, and turbidity method.

A summary of the results is shown in Table 10.A.

The different modes were compared as follows:

1-First mode based on comparison between the practical value (i.e., $\bar{W}_i$) and the official value [47–52] (µ= 4 mg), which is based on the following hypotheses:

$H_\circ = \mu_{(4mg)} = \bar{w}_i$ (for all companies)

against the alternative hypothesis

$H_1 = \mu_{(4mg)} \neq \bar{w}_i$ (for all companies)

Table 10.B shows that the calculated t-value was less than the tabular t-value (4.303) for all companies supplying the drug, indicating no significant difference between the practical value and the official value for all three samples.

2- The advanced methodology for CFIA and the classical method were compared to measure the absorbance at the UV region (λ_{max} = 265 nm) and turbidity, neglecting the difference between companies that produce the drugs of CPM and based upon the following assumption:

Null hypothesis $H_\circ = \mu_{NAG\text{-}SSP\text{-}5S\text{-}1D} = \mu_{UV\text{-}SP} = \mu_{turbidity}$ For three drugs

No significant difference exists between the mean of three methods.

Against

Alternative hypothesis: A significant difference exists between the mean of the classical method and the NAG-SSP-5S-1D analyzer i.e., $H_1 = \mu_{NAG\text{-}SSP\text{-}5S\text{-}1D} \neq \mu_{UV\text{-}SP} \neq \mu_{turbidity}$ (for all drugs)

Table 10.B indicates no significant difference among the three methods at 95% (α = 0.05). The calculated t_{cal} (2.430) was less than the t_{tab} (4.303) for the determination of CPM via UV spectrophotometry in different drugs. The t_{cal} (−0.7136) was less than the t_{tab}(4.303) for CPM with turbidity.

3- F-test by x one way-ANOVA was applied.

F-test was conducted to compare the four methods represented by the following assumption:

The null hypothesis ($\mu_{NAG\text{-}SSP\text{-}5S\text{-}1D} = \mu_{UV\text{-}SP} = \mu_{turbidity} = \mu_{officiall\ method}$) is no difference exists among the four methods. The alternative hypothesis is $\mu_{NAG\text{-}SSP\text{-}5S\text{-}1D} \neq \mu_{UV\text{-}SP} \neq \mu_{turbidity} \neq \mu_{officiall\ method}$.

At least one mean is different from others.

No significant differences were found among the four methods via accepting the original hypothesis, proving that the developed method was not affected by the interfering species available within the tablet. Therefore, it can be used as an alternative method, as reference or classic, because it is fast, consumes less chemical, and has high sensitivity by directing towards low concentrations, in addition to reliability when repeating results, whether on the same day or on successive days.

Table 10.A: Results for CPM using three methods.

Commercial Name, Company Content Country	Confidence interval For the average weight of Tablet $\bar{w}_i \pm 1.96\ \sigma_{n-1}/\sqrt{n}$ at 95% (g)	Type of method				
		Developed method of CPM-Sodium nitroprusside				
		UV-Spectrophotometer at λmax = 265 nm.				
		Turbidity method				
		Weight of Sample equivalent to 0.07818 g (2 mmol.L -1) of	Theoretical content for the active ingredient at 95% (mg) $W_i \pm 1.96\ \sigma_{n-1}/\sqrt{n}$	[CPM] mmol.L^{-1}	Equation of standard addition at 95% confidence level for n-2	r, r^2, R^2%

3.Chlomal Bioner 4 mg Iraq	2.Chlorohistol Julphar 4 mg U.A.E			1.Histadine SDI 4mg Iraq				
0.1134±0.0004	0.1106±0.001			0.1215±0.0009				
2.2164	2.1617			2.3747				
4 ±0.014	4 ±0.036			4 ±0.0296				
37	90	0.31	45	90	0.29	42	0	0 ml
245	140	0.51	300	135	0.48	275	2	0.4 ml
430	188	0.64	550	188	0.54	488	4	0.8 ml
590	230	0.82	778	230	0.75	730	6	1.2 ml
800	278	0.98	990	275	0.91	900	8	1.6 ml
46.2±36.256+93.55±7.401 [CPM]mmol.L-1	92±5.901+466±24.094 [CPM]mmol.L-1	0.322±0.041+1.650±0.169[CPM]mmol.L-1	59±41.554+118.4±8.483 [CPM]mmol.L-1	90.6±7.354+465±30.019 [CPM]mmol.L-1	0.292±0.095+1.51 ±0.391[CPM]mmol.L-1	52.8±50.591+108.55±10.326 [CPM]mmol.L-1	$\hat{Y}_{zi}$=a± S_at +b ± S_b t [CPM] mmol.L^{-1}	Ŷzi (mV)=a± Sat +b ± Sb t [CPM] mmol.L-1
0.9991,0.9982,99.82	0.9996,0.9992,99.92	0.9985,o.9969,99.69	0.9992,0.9984,99.84	0.9993,0.9988,99.88	0.9903,0.9806,98.06	0.9987,0.9973,99.73		

85	0.26
125	0.43
170	0.51
208	0.64
250	0.81
85±4.098+413±16.734 [CPM]mmol.L-1	0.268±0.067+1.31 ±0.270[CPM]mmol.L-1
0.9998,0.9995,99.95	0.9937,0.9874,98.74

Ŷzi: Estimated response in mV for developed method and without unit for UV spectrophotometry and turbidity method, r: correlation coefficient, r2: coefficient of determination, R2% (percentage capital R-squared): explained variation as a percentage /total variation.

Table 4.10.B: Summary of results for practical content, (Rec. %): efficiency for determination of CPM in three samples of drugs and t-test for comparison among three methods (paired t-test or individual t-test).

1					No. of sample			
1.934	0.1934	0.0761	1.9457	0.4864	Practical weight of CPM w̄i(g)	Practical concentration (mmol.L-1) in 100ml	Practical concentration (mmol.L-1) in 10ml	Type of method Developed method of CPM-Sodium nitroprusside UV-Spectrophotometer at λmax=265nm. Turbidity method
0.0756		3.8913± 1.285	0.0761		Weight of CPM in each drug w̄i(mg)±4.303σn-1/√n		Weight of CPM in each weight of sample w̄i(g)	
96.69		97.28			Efficiency of determination Rec.%			
/-0.3642/ <<ttab(4.303)					Individual t-test for compared between quoted value & practical value (w̄i(g)-µ) √n/ σn-1			
Newly developed CPM-Nitro press & UV-Spectrophotometer methods W̄d = 0.0825 σ^*_{n-1}= 0.0588 2.430 << 4.303					tcal=w̄d √n/σ*n-1		Paired t-test for compared between two methods	
					ttab at 95% confidence level at n-1			

3									**2**												
0.0805	**2.0581**	**0.2058**	**0.0799**	**2.0458**	**0.205**	**0.0772**	**1.9754**	**0.4939**	**0.0772**	**1.9742**	**0.1974**	**0.0763**	**1.9515**	**0.1952**	**0.0779**	**1.9932**	**0.4983**	**0.0762**	**1.9485**	**0.1948**	**0.0756**
4.116±0.528	**0.0805**		**4.0916±0.921**	**0.0799**		**3.9508±1.874**		**0.0772**	**3.949±1.582**		**0.0772**	**3.903±0.982**	**0.0763**		**3.9865±1.981**		**0.0779**	**3.897±1.883**		**0.0762**	**3.868±1.025**
102.91			**102.29**			**98.77**			**98.71**			**97.58**			**99.66**			**97.42**			
/-0.1130/ <<ttab(4.303)									**/-0.0293/ <<ttab(4.303)**												
Newly developed CPM-Nitro press and Turbidimetry methods $\bar{W}d = -0.044$ $\sigma^{*}_{n-1} = 0.1068$ /-0.7136/<< 4.303																					

μ: quoted value, $\bar{x}$d: average of difference among three methods (developed and classical (UV spectrophotometry and turbidity), n: (no. of sample) = 3, σ_{n-1}: standard deviation of different (paired t-test), $\bar{w}_i$: practically weight in g, $t_{tab} = t_{0.05/2,2} = 4.303$ (for individual t-test and paired-t test).

Conclusion

CPM was assessed through its reaction with Nitropress, which led to the formation of pale white colored complex. The homemade NAG-SSP-5S-1D solar cell CFI analyzer was used for the measurement of attenuation of incident light by using five sources of WSLED located at 0°–180° relative to the detector . The new technique was very simple, sensitive and applied successfully for assessment of different metals ion such as CPM in three different drugs. This research presents a new and innovative design (NAG-SSP-5S-1D analyzer) that has many industrial and environmental applications, with measurements characterized by reliability, repeatability, and high confidence. One of its applications is noted in the determination of CPM at concentrations reaching microgram (0.0328 µg/sample), with120 µl as a sample segment. The flow cell is provided in its entirety. Its manufacture is possible because it was established in a home workshop by one of the researchers. In addition, the detector does not need amplification nor signal purification circuits due to the responses being free of electronic noise, as shown by the purity of the obtained responses.

Acknowledgment

The author thank Prof. Dr. Issam Al-Hashimi for his support

References:

[1] Walsh, G. M. (2012). Antihistamines (H1 receptor antagonists). In *Side Effects of Drugs Annual* (Vol. 34, pp. 271-276). Elsevier.

[2] Meltzer, E. O., Berman, G. D., Corren, J., Pedinoff, A. J., Doyle, G., Waksman, J. A., ... & Wason, S. (2004). Addition of ibuprofen to pseudoephedrine and chlorpheniramine in the treatment of seasonal allergic rhinitis. *Annals of Allergy, Asthma & Immunology*, *93*(5), 452-459.

[3]Samaneh Nakhaee [a], Omid Mehrpour [b],2023, Chlorpheniramine, Reference Module in Biomedical Sciences.

[4] Moyer, R. A., Sidell, F. R., & Salem, H. (2014). Encyclopedia of toxicology.

[5] Kumari, R., Kumari, R., & Bais, S. (2020). Combined effect of Cromolyn sodium and Chlorpheniramine Maleate in high fat diet induced obesity. *Obesity Medicine*, *18*, 100218.

[6] Aït Moussa, L., Tebaa, A., Alj, L., Sefiani, H., Meski, F. Z., Khattabi, A., & Soulaymani

Bencheikh, R. (2023). Adverse drug reactions to chloroquine/hydroxychloroquine in combination with azithromycin in COVID-19 in-patients: data from intensive pharmacovigilance in Morocco, 2020. *Naunyn-Schmiedeberg's Archives of Pharmacology*, *396*(12), 3847-3856.

[7] Landau, R., Achilladelis, B., & Scriabine, A. (Eds.). (1999). *Pharmaceutical innovation: revolutionizing human health* (Vol. 2). Chemical Heritage Foundation.

[8] Motomizu, S., & Sakai, T. (2008). On-line sample pretreatment: extraction and preconcentration. In *Comprehensive Analytical Chemistry* (Vol. 54, pp. 159-201). Elsevier.

[9] Xu, W., Sandford, R. C., Worsfold, P. J., Carlton, A., & Hanrahan, G. (2005). Flow injection techniques in aquatic environmental analysis: Recent applications and technological advances. *Critical reviews in analytical chemistry*, *35*(3), 237-246.

[10] Turkey, N. S., & Mezaal, E. N. (2020). Continuous flow injection analysis, turbidmetric and photometric determination of methyldopa drugs using a new long distance chasing photometer (NAG-ADF-300-2). *Indian Journal of Forensic Medicine & Toxicology*, *14*(4), 1495.

[11] Al-Ani, Asma A. Gayed, and Nagham S. Turkey Al-Awadie.(2025) "Continuous Flow Injection: Turbidimetric (0-180) Determination of Chlorpheniramine Maleate Using Five Snow White LEDs as a Source of Irradiation and Single Solar Cells as an Energy Transducer. Advanced Journal of Chemistry, Section A, 8(3), 469-494.

[12] Turkie, N. S., & Hameed, S. F. (2022). Continuous flow injection analysis via NAG-4SX3-3D analyzer utilized to determination of resorcinol. *Asian Journal of Green Chemistry*, *6*, 129.

[13] Turkie, N. S., & Hameed, S. F. (2022). Determination of Fuconazole Using Flow Injection Analysis and Turbidity Measurement by a Homemade NAG-4SX3-3D Analyzer.

[14] Shakir, I. M., & Mansoor, A. A. (2014). A New Approach for the Turbidimetric Determination of Hydronium ion by Using Homemade Linear Array Ayah 5SX1-T-1D-CFI Analyser. *Iraqi Journal of Science*, 1751-1769.

[15] Shakir, I. (2014). New turbidimetric-continuous flow injection analysis method for the determination of chlorpromazine HCl in pharmaceutical preparation using linear array ayah 5SX1-T-1D-CFI analyser. *Iraqi Journal of Science*, *55*(2B), 594-605.

[16] Al-Awadie, N. S. T., & Al-saadi, K. H. I. (2015). Turbidimetric determination of metoclopramide hydrochloride in pharmaceutical preparation via the use of a new homemade Ayah 6SX1-T-2D solar cell-continuous flow injection analyser. *Iraqi journal of science*, 1224-1240.

[17] Masood, S., Khan, Z., Ashfaq, M., & Khan, S. R. (2020). Optical studies of acefylline piperazine, chlorpheniramine maleate, thiamine hydrochloride in aqueous, aqueous methanol and aqueous ethylene glycol systems. *Journal of Molecular Liquids*, *303*, 112611.

[18] Pourghobadi, Z., & Pourghobadi, R. (2015). Electrochemical behavior and voltammetric determination of chlorpheniramine maleate by means of multiwall carbon nanotubes-modified glassy carbon electrode. *International Journal of Electrochemical Science*, *10*(9), 7241-7250.

[19] Acheampong, A., Gyasi, W. O., Darko, G., Apau, J., & Addai-Arhin, S. (2016). Validated RP-HPLC method for simultaneous determination and quantification of chlorpheniramine maleate, paracetamol and caffeine in tablet formulation. *Springerplus*, *5*, 1-8.

[20] Aldewachi, H., & Omar, T. A. (2022). Development of HPLC Method for Simultaneous Determination of Ibuprofen and Chlorpheniramine Maleate. *Scientia Pharmaceutica*, *90*(3), 53.

[21] Sanchaniya, P. M., Mehta, F. A., & Uchadadiya, N. B. (2013). Development and validation of an RP-HPLC method for estimation of chlorpheniramine maleate, ibuprofen, and phenylephrine hydrochloride in combined pharmaceutical dosage form. *Chromatography Research International*, *2013*.

[22] Zahoor, A., Munir, H., Junaid, R., Hussain, S., Naveed, S., Alam, M. O., ... & Khan, S. (2018). A RP-HPLC Method for Simultaneous estimation of Chlorpheniramine Maleate, Paracetamoland Phenylephrine Hydrochloride in Bulk. *RADS Journal of Pharmacy and Pharmaceutical Sciences*, *6*(1), 53-58.

[23] Sirigiri, B., Chengalva, P., Parameswari, S. A., & Aruna, G. (2018). A novel HPLC method for the simultaneous determination of chlorpheniramine maleate and dextromethorphan in bulk and pharmaceutical formulation. *Int. J. Pharm. Sci. Res*, *9*, 1147-1151.

[24] Redasani, V. K., Gorle, A. P., Badhan, R. A., Jain, P. S., & Surana, S. J. (2013). Simultaneous determination of chlorpheniramine maleate, phenylephrine hydrochloride, paracetamol and caffeine in pharmaceutical preparation by RP-HPLC. *Chemical Industry and Chemical Engineering Quarterly/CICEQ*, *19*(1), 57-65.

[25] Qi, M. L., Wang, P., Leng, Y. X., Gu, J. L., & Fu, R. N. (2002). Simple HPLC method for simultaneous determination of acetaminophen, caffeine and chlorpheniramine maleate in tablet formulations. *Chromatographia*, *56*, 295-298.

[26] Kaura, A. K., Gupta, V., Kaura, M., Roy, G. S., & Bansal, P. (2013). Spectrophotometric determination of Chlorpheniramine Maleate and Phenylpropanolamine Hydrochloride by "two wavelengths method". *journal of pharmacy research*, *7*(5), 404-408.

[27] Hussein, N. G., & Saeed, A. M. (2021). Simultaneous estimation of chlorpheniramine maleate and glyceryl guaiacolate in pure and capsule dosage form by using different spectrophotometric methods. *Research Journal of Pharmacy and Technology*, *14*(5), 2608-2612.

[28] Mahmoud, A. R., & Al-Healy, F. M. (2021). UV-Spectral studies on chlorpheniramine maleate in pure form and pharmaceutical preparations. *Egyptian Journal of Chemistry*, *64*(8), 4151-4156.

[29] Mishra, K., Kumar, B. K., Kumari, M. M., & Subrahmanyam, B. S. S. (2016). New analytical method development and validation of chlorpheniramine maleate by using uv-visible spectrophotometry. *Indo American Journal of Pharmaceutical Sciences*, *3*(7), 767-772.

[30] Rita B. Prajapati1, Priya B. Patel , Rajvi Mahida, 2019, Spectrophotometric Determination of Chlorpheniramine Maleate in its Pharmaceutical Dosage form using Quality by Design Approach, J Pharm Sci Bioscientific Res, pp: 260-267.

[31] Kaura, A. K., Sharma, R., Monika, P. B., & Chawla, R. SPECTROPHOTOMETRIC DETERMINATION OF CHLORPHENIRAMINE MALEATE AND PHENYLPROPANOLAMINE HYDROCHLORIDE USING "MULTIWAVELENGTH SPECTROSCOPIC METHOD".

[32] Al-Shaalan, N. H. (2010). Determination of phenylephrine hydrochloride and chlorpheniramine maleate in binary mixture using chemometric-assisted spectrophotometric and high-performance liquid chromatographic-UV methods. *Journal of Saudi Chemical Society*, *14*(1), 15-21.

[33] Yu, C., Tang, Y., Han, X., & Wu, S. (2006). Flow injection chemiluminescence analysis of diphenhydramine hydrochloride and chlorpheniramine maleate. *Instrumentation Science and Technology*, *34*(5), 529-536.

[34] Koibuchi, M., & Ejima, A. (1979). Determination of pharmaceutical preparations by gas chromatography. V. Determination of chlorpheniramine maleate and dl-methylephedrine hydrochloride using a nitrogen selective RbCl-alkali flame ionization detector. *Eisei Kagaku*, *25*, 295-300.

[35] Alghazal, M. E. K., Alrouh, F., Bitar, Y., & Trefi, S. (2019). Determination of Dimenhydrinate and Chlorpheniramine Maleate in Pharmaceutical Forms by new Gas Chromatography Method. *Research Journal of Pharmacy and Technology*, *12*(6), 2851-2856.

[36] Fontan, C. R., Smith, W. C., & Kirk, P. L. (1963). Gas Chromatography of the Antihistamines. *Analytical Chemistry*, *35*(4), 591-591.

[37] Harsono, T., Yuwono, M., & Indrayanto, G. (2005). Simultaneous determination of some active ingredients in cough and cold preparations by gas chromatography, and method validation. *Journal of AOAC international*, *88*(4), 1093-1098.

[38] Yang, F., Duan, X., Wang, Z., & Dong, Y. (2022). A gas chromatography flame ionization detector method for rapid simultaneous separation and determination of six active ingredients of anticold drug. *Current Pharmaceutical Analysis*, *18*(1), 71-81.

[39] Moyano, M. A., Rosasco, M. A., Pizzorno, M. T., & Segall, A. I. (2005). Simultaneous determination of chlorpheniramine maleate and dexamethasone in a tablet dosage form by liquid

chromatography. *Journal of AOAC International*, *88*(6), 1677-1683.

[40] Takagaki, T., Matsuda, M., Mizuki, Y., & Terauchi, Y. (2002). Simple and sensitive method for the determination of chlorpheniramine maleate in human plasma using liquid chromatography–mass spectrometry. *Journal of Chromatography B*, *776*(2), 169-176.

[41] Eldawy, M. A., Mabrouk, M. M., & El-Barbary, F. A. (2003). Determination of chlorpheniramine maleate and tincture ipecac in dosage form by liquid chromatography with ultraviolet detection. *Journal of AOAC International*, *86*(4), 675-680.

[42] Hadad, G. M., El-Gindy, A., & Mahmoud, W. M. (2007). Development and validation of chemometrics-assisted spectrophotometry and liquid chromatography methods for the simultaneous determination of the active ingredients in two multicomponent mixtures containing chlorpheniramine maleate and phenylpropanolamine hydrochloride. *Journal of AOAC International*, *90*(4), 957-970.

[43] IRQ. PATENT . No. 7685. Shakir ,I.M.A. and Al-Awadie ,N.S.T., Simplified Sensitive Portable one raw matrix cell photometer for continuous ON-Line flow analysis)NAG – SSP (, .2022, patent, International classification G01N11/00 , F15D1/00 , G05D7/00.

[44] SATYA PRAKASH, G.D.TULI, S.K.BASU, R.D.MADAN, Advanced inorganic chemistry, Ram Nager, new delhi, 2000, vol.1, pp; 110055.

[45] Chawe, L. C. D., Tittikpina, N. K., Ndiaye, S. M., Diop, A., Ndiaye, B., Fall, D., ... & Sarr, S. O. (2021). Validation of an UV-Visible spectrophotometry assay method for the determination of chlorpheniramine maleate tablets without prior extraction. *International Journal of Biological and Chemical Sciences*, *15*(1), 273-281.

[46] PARACETAMOL, V. O., & MALEATE, C. INTERNATIONAL RESEARCH JOURNAL OF PHARMACY.

[47] Agnew, T. M., Irvine, R. O. H., & North, J. D. K. (1963). Methyldopa and hydrochlorothiazide compared with reserpine and hydrochlorothiazide in hypertension. *British Medical Journal*, *2*(5360), 781.

[48] British pharmacopoeia. 2012. 7 th Ed. The Stationery office. London.

[49] Pharmacopoeia B. 3013. British pharmacopoeia commission London; the department of health. Social Services and Public Safety.

[50] Pharmacopoeia, B. (2003). The Stationary Office Ltd. *Crown Copyright*, *388*.

[51] Hoyle, M. (2008). Future drug prices and cost-effectiveness analyses. *Pharmacoeconomics*, *26*, 589-602.

[52] Griffin, J. P. (2009). 17 History of drug regulation in the UK. *The Textbook of Pharmaceutical Medicine*, 413.

P- ISSN 1991-8941 E-ISSN 2706-6703 Journal of University of Anbar for Pure Science (JUAPS) Open Access
2025,(19), (01):174 – 190

التحليل شبه التلقائي للتقدير النانوي لعقار الكلوروفينرايمين ماليت بأستخدام نايتروبروسيد الصوديوم وبوساطة التغذية المستمرة بالجريان لفوتوميتر بسيط وحساس متنقل مصمم محليا

نغم شاكر تركي العوادي ،اسمه عادل كعيد العاني*

قسم علوم الكيمياء، كلية العلوم، جامعة بغداد، بغداد، العراق
email: asma.alani.16@gmail.com

الخلاصة:

تقدم هذه الدراسة نهجا سريعا وحساسا ومباشرا لقياس الكلورفينيرامين ماليت (CPM) باستخدام التعكريه– CFIA. تتضمن الطريقة تفاعل CPM مع نيتروبروسيد الصوديوم (nitropress) لإنتاج راسب أبيض شاحب. للكشف عن توهين الضوء الساقط نتيجة الاصطدام على أسطح الجسيمات المترسبة، تم استخدام المحلل NAG–SSP–5S–1D لقياس التعكريه بزاوية (0–180°).

يمتد النطاق الخطي لقياسات CPM من 0.008 إلى 11 مللي مول\لتر مع معامل ارتباط 0.9983 و R^2% = 99.65. تم تحديد حد الكشف (LOD) ليكون 0.0328 ميكروجرام\عينة من أقل تركيز مخفف في المعايرة المنحنى، وتبين أن تكرار الطريقة (RSD%) أقل من 0.4% (n=6) للتركيز المحدد (10,13 مللي مول\لتر). تم تطبيق الطريقة بنجاح لتحديد CPM في مجموعة متنوعة من الأدوية باستخدام طريقة الإضافة القياسية. تم إجراء مقارنة بين طريقة التحليل المطورة حديثاً والطريقة التقليدية ((قياس الطيف الضوئي للأشعة فوق البنفسجية عند λ_{max}= 265nm والعكارة) باستخدام اختبار t. وقد لوحظ عدم وجود فروق معنوية بين الطرق الثلاث عند مستوى ثقة 95%. توفر طريقة حقن التدفق المطورة البساطة والحساسية والأداء التحليلي الموثوق به لتحديد CPM، لذلك يمكن استخدام الطريقة المطورة حديثًا كطريقة بديلة ومقبولة لتحليل CPM في الأدوية مقارنة بالطريقة المرجعية.

الكلمات المفتاحية :التحليل بالتدفق الجرياني المستمر، التعكرية ،نيتروبروسيد الصوديوم، كلورفينيرامين ماليت، المحلل NAG–SSP–5S–1D ،طريقة المقياس الطيفي.